NANO LETTERS

pubs.acs.org/NanoLett

Charge Noise in Graphene Transistors

Iddo Heller,[†,§] Sohail Chatoor,[†] Jaan Männik,[†] Marcel A. G. Zevenbergen,[†] Jeroen B. Oostinga,[†,‡] Alberto F. Morpurgo,[†,‡] Cees Dekker,[†] and Serge G. Lemay*[,†,||]

[†] Kavli Institute of Nanoscience, Delft University of Technology, Lorentzweg 1, 2628 CJ Delft, The Netherlands, and [‡] DPMC and GAP, University of Geneva, quai Ernest-Ansermet 24, CH-1211 Geneva 4, Switzerland

ABSTRACT We report an experimental study of 1/*f* noise in liquid-gated graphene transistors. We show that the gate dependence of the noise is well described by a charge-noise model, whereas Hooge's empirical relation fails to describe the data. At low carrier density, the noise can be attributed to fluctuating charges in close proximity to the graphene, while at high carrier density it is consistent with noise due to scattering in the channel. The charge noise power scales inversely with the device area, and bilayer devices exhibit lower noise than single-layer devices. In air, the observed noise is also consistent with the charge-noise model.

KEYWORDS Graphene, liquid gate, transistor, 1/*f* noise, Hooge, charge noise

Inherent noise limits the performance of electronic devices in circuits and sensors. Here we focus on graphene, which has been shown to function as a promising sensor material in both the gas phase[1] and the liquid phase.[2] The sensing mechanism of these devices relies on local perturbations of the graphene sheet that modulate its global transport properties[1,3] in a manner analogous to the field effect induced by a gate electrode.[4] An exceptionally high sensitivity to adsorbed gas species was demonstrated, even down to single-molecule sensitivity.[1] When employed in liquid, carbon field-effect devices based on carbon nanotubes, graphene, and chemically modified graphene can be used as sensors for dissolved species such as charged biomolecules.[3,5−7] Because of the high sensitivity to local perturbations, it is expected that uncontrolled charge fluctuations in the vicinity of the device - as commonly associated with charge traps in the silicon oxide substrate[8] - can result in considerable low-frequency noise, which is detrimental to device performance. To date, few studies have addressed the noise properties of graphene. In the low-frequency limit, where sensing experiments are typically performed, graphene exhibits a 1/*f*-type noise spectrum.[8,9] A recent report on 1/*f* noise of graphene nanoribbons in vacuum[8] suggests that single-layer graphene (SLG) obeys the empirical Hooge relation,[10] whereas bilayer graphene (BLG) exhibits a suppression of the noise. No report has so far addressed the noise properties of liquid-gated graphene, the configuration most relevant for liquid-phase sensing.

In this letter, we present an experimental study of 1/*f* noise in liquid-gated SLG and BLG devices. In particular, we address the scaling of the noise properties with the gate voltage, the device dimensions, and the number of graphene layers. We find that the dependence of the noise on the gate-induced carrier density qualitatively disagrees with the Hooge relation. Instead, our experimental observations are consistent with an augmented charge-noise model,[11−13] which distinguishes between two separate contributions to the noise. At low carrier density, the noise is dominated by charge noise associated with random charge fluctuations in the environment that couple to the device through a field effect. This charge noise scales inversely with the device area and is lower for BLG than for SLG devices. At high carrier density, a gate-independent noise source becomes apparent that can be associated with scattering in the channel. These findings are consistent with the augmented charge-noise model and previous observations of charge noise in liquid-gated carbon nanotube devices.[12,13]

Two-terminal graphene devices were prepared from mechanically exfoliated graphite on oxidized silicon wafers (285 nm SiO_2).[4] The graphene flakes were identified by their optical contrast[14] and electrically contacted with Cr/Au electrodes patterned using e-beam lithography. Measurements were performed in a home-built flow cell[13] filled with an aqueous electrolyte buffered at pH 7.2 using 10 mM phosphate buffer. A liquid-gate potential, V_{lg}, was applied to an Ag/AgCl (3 M NaCl) reference electrode[15] inserted in the flow cell. In such an electrolyte-gated configuration, the device is gated by a field effect from mobile ions that form an electrical double-layer in solution.[16−20]

Figure 1a depicts graphene in a liquid-gated transistor layout. We measured the source-drain current, I_{sd}, while applying a small dc bias voltage V_{sd} (≤5 mV). All electrical measurements were performed as described in ref 12. Figure 1b shows typical source-drain conductance $G(V_{lg})$ curves measured for liquid-gated SLG and BLG devices. The curves exhibit a minimum in $G(V_{lg})$ at the Dirac point, and a monotonically increasing $G(V_{lg})$ on both sides away from the Dirac point.[21,22] We measured current-noise power spectra,

* To whom correspondence should be addressed. E-mail: S.G.Lemay@utwente.nl.

§ Present address: Department of Physics and Astronomy, VU University, De Boelelaan 1081, 1081 HV Amsterdam, The Netherlands.

|| Present address: MESA+ Institute and Faculty of Science and Technology, University of Twente, P.O. Box 217, 7500 AE Enschede, The Netherlands.

Received for review: 11/3/2009
Published on Web: 04/07/2010

DOI: 10.1021/nl903665g | *Nano Lett.* **2010,** *10,* 1563–1567

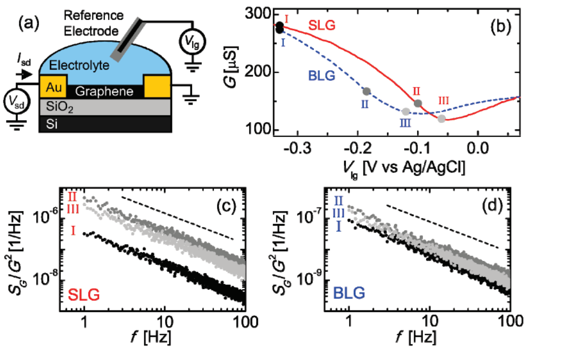

FIGURE 1. (a) Device schematic of a liquid-gated graphene transistor. (b) Source-drain conductance, G, vs liquid-gate voltage, V_{lg}, for a SLG (solid line) and a BLG (dashed line) device. (c,d) Normalized conductance-noise power spectra $S_G/G^2(f)$ for the SLG and BLG devices of (a) respectively. The spectra were obtained at values of V_{lg} as indicated by the dots labeled I, II, and III in (b). Dashed lines indicate $1/f$ slopes.

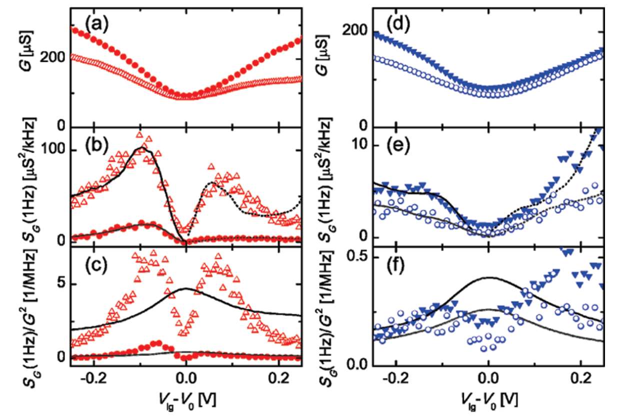

FIGURE 2. (a) Conductance, G, vs gate voltage, $V_{lg} - V_0$, for two SLG devices. V_0 is the liquid-gate voltage where G is mimimal and corresponds to the Dirac point. (b) Conductance noise power at 1 Hz, S_G(1 Hz), vs gate voltage. The curves represent the augmented charge-noise model separately fitted to the data for $V_{lg} < V_0$ and $V_{lg} > V_0$. For plotting purposes the fits have been smoothed; see Supporting Information, Figure S1 for unsmoothed fits. (c) Normalized noise amplitude S_G(1 Hz)/G^2 vs gate voltage. The curves represent best fits to the Hooge model. (d−f) Same as (a−c) but for two BLG devices.

$S_I(f)$ as function of V_{lg}. Figure 1c,d plots the normalized conductance-noise power spectra, $S_G(f)/G^2 = S_I(f)/I_{sd}^2$, for the SLG and BLG devices of Figure 1b, respectively. Power spectra are shown for three different gate voltages, as indicated in Figure 1b (grayscale dots labeled I−III). Strikingly, for both the SLG and the BLG device, the noise power does not increase monotonically with increasing $|V_{lg}|$. Instead the noise power exhibits a maximum at intermediate carrier density (II) where dI_{sd}/dV_{lg} is largest. This gate dependence of the noise power is indicative of charge noise, as discussed below.[11,12]

To study in detail the dependence of the $1/f$ noise on the number of gate-induced charge carriers, we characterized the noise as a function of V_{lg} for thirteen SLG and seven BLG devices. Figure 2 presents typical transport and noise data for two SLG devices (Figure 2a−c), and two BLG devices (Figure 2d−f). In Figure 2a,d, the conductance G for each device is plotted as function of the gate voltage. To facilitate comparison between different devices, the V_{lg} axes have been centered at V_0, defined as the gate voltage at which G is minimum. We recorded the noise power spectrum at each gate voltage and, as a representative measure for the magnitude of the low-frequency noise, we extracted the conductance noise power spectral density at 1 Hz, S_G(1 Hz) $= S_I(1\ \text{Hz})/V_{sd}^2$, by fitting $S_I(f) = S_I(1\ \text{Hz})/f^{\beta}$ to each spectrum. Typically, the fitted noise exponent β was $0.8 \leq \beta \leq 1.2$. Figure 2b,e shows S_G(1 Hz) for the devices of Figure 2a,d, respectively. S_G(1 Hz) is clearly at a minimum value at V_0. Away from V_0, S_G(1 Hz) passes through a maximum before decreasing again for the SLG devices, whereas it continues to increase or appears to saturate for the BLG devices.

We first compare the gate dependence of low-frequency noise to the empirical Hooge model, which states that the normalized low-frequency noise amplitude, $S_G(f)/G^2$, is inversely proportional to the number of charge carriers. Following the arguments of ref 8, Hooge's relation predicts that $S_G(f)/G^2$ is approximately proportional to the device resistance, G^{-1}. To facilitate a comparison of the noise to the Hooge model, Figure 2c,f shows the normalized noise amplitude at 1 Hz, $S_G(1\ \text{Hz})/G^2$, for the devices of Figure 2b,e, respectively. Similar to S_G(1 Hz), the experimental data for $S_G(1\ \text{Hz})/G^2$ exhibit a minimum at V_0 and passes through a local maximum negative of V_0. Comparing the Hooge prediction $S_G(1\ \text{Hz})/G^2 = \zeta/G$ to the data in Figure 2c,f (solid lines), where ζ is treated as an adjustable parameter, it is clear that the gate dependence of the noise in liquid-gated graphene devices cannot be described by Hooge's relation. Whereas Hooge's model predicts a maximum in $S_G(1\ \text{Hz})/G^2$ at the Dirac point, where the carrier density is minimum, we instead observe a pronounced minimum in $S_G(1\ \text{Hz})/G^2$ for both SLG and BLG devices.

Alternatively, we compare the data to an augmented charge-noise model proposed by Tersoff,[11] which we recently used to successfully describe $1/f$ noise in liquid-gated carbon nanotube transistors.[12,13] The augmented charge-noise model predicts that $S_I(1\ \text{Hz}) = V_{sd}^2 S_G(1\ \text{Hz}) = S_{input}(dI_{sd}/dV_{lg})^2 + A_S(R_S/R_{tot})^2 I_{sd}^2$. Here the first (charge-noise) term represents current noise associated with random charge fluctuations with power S_q in the vicinity of the device. These charge fluctuations couple to the transistor with an effective gate capacitance C_{gate} and can thus be represented as random voltage fluctuations of the gate potential[12] with power $S_{input} = (1/C_{gate})^2 S_q$. The second term of the augmented charge-noise model represents current noise from a gate-independent series resistance R_S that exhibits $1/f$ noise with a noise amplitude $A_S = \alpha_S(V_{sd}/R_S)^2$, such that the total contribution equals $A_S(R_S/R_{tot})^2 I_{sd}^2 = \alpha_S I_{sd}^4$.[13] The curves in Figure 2b,e are fits of the charge-noise model to the S_I(1 Hz) data (with S_{input} and α_S as fit parameters). To minimize the influence of any residual hysteresis, dI_{sd}/dV_{lg} was determined by measuring I_{sd} at V_{lg} and at $V_{lg} \pm \Delta V$ (with $\Delta V \leq 10$ mV) and calculating

DOI: 10.1021/nl903665g | Nano Lett. 2010, 10, 1563–-1567

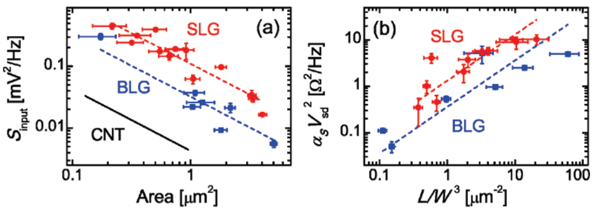

FIGURE 3. (a) S_{input} vs graphene Area. The dashed lines represent separate 1/Area fits to the SLG and BLG data. The black solid line indicates the 1/Area trend for CNTs as obtained from ref 12. (b) $\alpha_S V_{sd}^2$ vs L/W^3. The dashed lines represent separate L/W^3 fits to the SLG and BLG data. S_{input} and α_S were obtained from fits of the augmented charge-noise model to the p region ($V_{lg} < V_0$).

$\Delta I_{sd}/\Delta V_{lg}$. Since the conductance and noise data exhibit significant electron–hole asymmetry, likely due to a pn junction that can form by doping from the contact, we fitted the p region ($V_{lg} < V_0$), and n region ($V_{lg} > V_0$) separately.

The augmented charge-noise model describes the data well for both SLG and BLG devices (cf. Figure 2b,e). Especially striking for the SLG devices, the charge-noise term captures both the minimum in S_I near the Dirac point and the maximum in S_I at intermediate carrier concentrations, where dI_{sd}/dV_{lg} has a maximum. This indicates that for SLG devices charge noise dominates the noise properties. Although we have also observed a similar dominance of charge noise for some BLG devices, more typically the noise at high carrier density in BLG devices is dominated by the series-resistor term, such that S_G increases monotonically with G, as in Figure 2e (see Supporting Information, Figures S2 and S3). This apparent difference is however consistent with the augmented charge-noise model, as discussed below. Finally, at the Dirac point, the augmented charge-noise model underestimates the measured noise power for both SLG and BLG devices (cf Figures 2b and 2e). This is at least in part due to the model neglecting high-order terms in the Taylor-expansion of $I_{sd}(V_{lg})$, which we have omitted for simplicity.

We now turn to the dependence of the noise parameters S_{input} and α_S on device dimensions. Figure 3a plots S_{input} (fitted on the p-side) as a function of device area for all measured SLG (red dots) and BLG devices (blue squares). Two features stand out. First, S_{input} exhibits a 1/Area dependence (dashed lines). This 1/Area dependence follows naturally from $S_{input} = (1/C_{gate})^2 S_q$, where both C_{gate} and S_q are expected to scale linearly with the graphene area (the latter corresponding to local, independent charge fluctuators that are evenly distributed over the graphene surface), yielding $S_{input} \propto 1/\text{Area}$. Second, SLG devices exhibit a higher S_{input} than BLG devices. We fitted the form $S_{input} = \xi/\text{Area}$ to the data in Figure 3a (dashed lines), yielding fitted values of $\xi_{SLG} = 0.11 \pm 0.01$ $\mu m^2 mV^2/Hz$ for SLG devices and $\xi_{BLG} = 0.032 \pm 0.005$ $\mu m^2 mV^2/Hz$ for BLG devices. We thus observe that the ratio $\xi_{SLG}/\xi_{BLG} = 3.4 \pm 0.6$. This difference between the charge-noise power for SLG and BLG devices can be understood by considering the effective gate capacitance between the fluctuating charges and the graphene. The intrinsic quantum capacitance C_q of the graphene sets an upper bound for the net gate capacitance C_g.[20] Since C_q per unit area for BLG is roughly twice that of SLG (ignoring for simplicity the gate dependence of the quantum capacitance, see Supporting Information), this implies that $\xi_{SLG}/\xi_{BLG} = (C_{g,BLG}/C_{g,SLG})^2 \leq (C_{q,BLG}/C_{q,SLG})^2 \approx 4$, in rough agreement with our experimental observations. This is consistent with charge traps near the surface of the oxide. Interestingly, it is also consistent with association/dissociation of charged moieties (silanol groups) on the surface of the oxide and/or of the graphene that result from chemical equilibrium with the aqueous solution, a mechanism that is unique to electrolyte gating. Finally, another source of fluctuations comes from mobile ions in solution diffusing near the graphene. Because the typical residence time of such an ion within a Debye screening length of the surface is of the order of nanoseconds, however, this is not expected to contribute significantly to the low-frequency noise studied here.

We can compare the charge noise of graphene to charge noise previously measured for carbon nanotubes (CNTs).[12] In ref 12, the length-corrected S_{input} for CNTs was found to be 0.54 $mV^2 \mu m/Hz$, which yields $\xi_{CNT} \approx 0.004$ $\mu m^2 mV^2/Hz$ (dotted line in Figure 3a), assuming an average CNT diameter of 2.5 nm. Strikingly, CNTs exhibit nearly 1 order of magnitude lower charge noise than BLG devices. This may be caused by the electrolyte that surrounds the CNT and screens out a large fraction of the charge fluctuations from the underlying substrate, suggesting that the dominant fluctuators are associated with the silicon oxide substrate rather than the graphene itself.

Next we analyze the geometry dependence of the $1/f$ noise of graphene at high carrier density. The fit parameter for the series-resistor term, which dominates noise at high carrier density, is $\alpha_S = A_S(R_S/V_{sd})^2 = S_R/V_{sd}^2$, where S_R is the resistance-noise power of the series resistor.[11] We assume for simplicity that R_S and S_R are independent of the gate voltage. The experimental scatter in our data however does not allow ruling out a weak gate dependence. Attributing the noise described by the series resistor term to mobility fluctuations caused by independent scatterers that are evenly distributed over the graphene sheet,[21-23] $\alpha_S V_{sd}^2$ is expected to scale as L/W^3, where L is the length, and W the width of the graphene (as derived in the Supporting Information). Figure 3b shows $\alpha_S V_{sd}^2$ as function of L/W^3, which is consistent with the data within experimental scatter. $\alpha_S V_{sd}^2$ is significantly larger for SLG than for BLG devices, which is expected if the density of fluctuating scatterers is the same in the two cases (as expected for oxide- or surface-bound scatterers) or scales linearly with the number of layers (as expected for lattice defects). Alternatively, we show in the Supporting Information Figure S4 that the scaling of $\alpha_S V_{sd}^2$ with geometry also appears consistent with a gate-independent contact resistance.[24,25] It is however unlikely that this is the dominant source of noise at high carrier density since the contact resistance was found to be independent of the

DOI: 10.1021/nl903665g | Nano Lett. 2010, 10, 1563–-1567

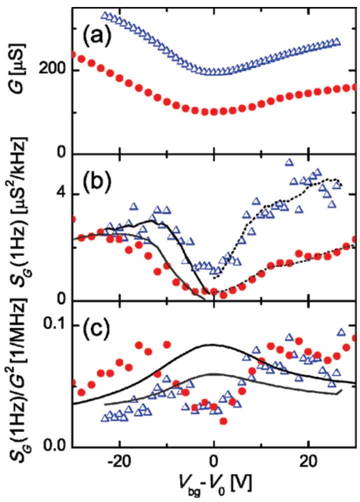

FIGURE 4. Noise measurements under ambient conditions. (a) Conductance, G, vs back-gate voltage, $V_{bg} - V_0$, for a SLG (red circles) and a BLG (blue triangles) device. (b) Conductance noise power at 1 Hz, S_G(1 Hz), vs gate voltage. The curves represent the augmented charge-noise model fitted to the data for $V_{lg} < V_0$ and $V_{lg} > V_0$. For plotting purposes, the fits have been smoothed; see Supporting Information, Figure S5 for unsmoothed fits. (c) Normalized noise amplitude S_G(1 Hz)/G^2 vs gate voltage. The curves represent fits to the Hooge model.

number of graphene layers,[25] whereas we find that $\alpha_S V_{sd}^2$ is significantly smaller for BLG than for SLG devices.

The suppressed noise for BLG devices that has been observed both here and in previous reports[8,9] can now be understood in terms of the augmented charge-noise model. First, BLG exhibits a lower gate modulation, dI_{sd}/dV_{lg}, and has roughly twice the quantum capacitance of SLG, both of which lead to a suppression of charge noise in BLG. In addition, we observed that the noise power of the series-resistor term is also suppressed for BLG devices (cf. Figure 3c), consistent with expectations for scatterers evenly distributed over the graphene.

Finally, we also measured the transport and low-frequency noise properties of graphene devices in ambient conditions in a back-gated transistor layout. Figure 4 plots the measured G, S_G(1 Hz), and S_G(1 Hz)/G^2 versus back-gate voltage V_{bg} for a SLG and a BLG device. Fitting the augmented charge-noise model and the Hooge relation to the data, as explained above, yields excellent agreement with our observations in liquid: the Hooge model fails to describe the back-gate data (cf. Figure 4c), whereas the augmented charge-noise model describes the noise well at all carrier densities except at the Dirac point (cf. Figure 4b). Our data differ from observations reported by Pal et al. and Lin et al.[8,9] It is likely that no contradiction exists, however, due to the different experimental configurations (in our measurements the graphene is exposed to ambient conditions instead of high vacuum or a top-gate dielectric consisting of PMMA).

Interestingly, direct comparison of individual devices measured both in liquid and in air indicates that the noise in liquid is higher than that in air (see Supporting Information, Figure S6), suggesting that the dominant fluctuators in liquid are dynamically associating/dissociating charged groups at the surface of the oxide.

In summary, we have studied the 1/*f*-noise properties of graphene in a liquid-gated transistor layout and have addressed the scaling of the noise properties with the gate-induced carrier density, the device dimensions, and the number of graphene layers. We find that the noise amplitude does not scale inversely with the number of gate-induced charge carriers as postulated by the empirical Hooge relation. Instead, for both SLG and BLG devices, the noise power is well described by an augmented charge-noise model, which reveals that at low carrier density the noise is dominated by charge noise that is associated with charge fluctuators in close proximity of the graphene sheet. The power of the charge noise scales inversely with the device area and the number of graphene layers. Interestingly, liquid-gated graphene exhibits a significantly higher charge-noise power in comparison to liquid-gated CNTs.

Acknowledgment. We acknowledge NWO and NanoNed for financial support.

Supporting Information Available. Fitted curves of Figures 2 and 4 without smoothing, additional noise data for a BLG device, analysis of noise associated with contact resistance, derivation of the scaling of $\alpha_S V_{sd}^2$ with device geometry, comparison of the noise in liquid and under ambient conditions, estimate of the ratio of quantum capacitances of SLG and BLG, and figures that show the relative contribution of charge-noise term and series resistor term to the fits of augmented charge noise model to data of Figure 2. This material is available free of charge via the Internet at http://pubs.acs.org.

REFERENCES AND NOTES

(1) Schedin, F.; Geim, A. K.; Morozov, S. V.; Hill, E. W.; Blake, P.; Katsnelson, M. I.; Novoselov, K. S. *Nat. Mater.* **2007**, *6*, 652.
(2) Ang, P. K.; Chen, W.; Wee, A. T. S.; Loh, K. P. *J. Am. Chem. Soc.* **2008**, *130*, 14392.
(3) Heller, I.; Janssens, A. M.; Männik, J.; Minot, E. D.; Lemay, S. G.; Dekker, C. *Nano Lett.* **2008**, *8*, 591.
(4) Novoselov, K. S.; Geim, A. K.; Morozov, S. V.; Jiang, D.; Zhang, Y.; Dubonos, S. V.; Grigorieva, I. V.; Firsov, A. A. *Science* **2004**, *306*, 666.
(5) Besteman, K.; Lee, J. O.; Wiertz, F. G. M.; Heering, H. A.; Dekker, C. *Nano Lett.* **2003**, *3*, 727.
(6) Mohanty, N.; Berry, V. *Nano Lett.* **2008**, *8*, 4469.
(7) Ohno, Y.; Maehashi, K.; Yamashiro, Y.; Matsumoto, K. *Nano Lett.* **2009**, *9*, 3318.
(8) Lin, Y. M.; Avouris, P. *Nano Lett.* **2008**, *8*, 2119.
(9) Pal, A. N.; Ghosh, A. *Phys. Rev. Lett.* **2009**, *102*, 126805.
(10) Hooge, F. N. *Phys. Lett. A* **1969**, *29*, 139.
(11) Tersoff, J. *Nano Lett.* **2007**, *7*, 194.
(12) Männik, J.; Heller, I.; Janssens, A. M.; Lemay, S. G.; Dekker, C. *Nano Lett.* **2008**, *8*, 685.
(13) Heller, I.; Männik, J.; Lemay, S. G.; Dekker, C. *Nano Lett.* **2009**, *9*, 377.

DOI: 10.1021/nl903665g | *Nano Lett.* **2010,** *10,* 1563–-1567

(14) Novoselov, K. S.; Jiang, D.; Schedin, F.; Booth, T. J.; Khotkevich, V. V.; Morozov, S. V.; Geim, A. K. *Proc. Nat. Ac. Sci. U.S.A.* **2005**, *102*, 10451.
(15) Minot, E. D.; Janssens, A. M.; Heller, I.; Heering, H. A.; Dekker, C.; Lemay, S. G. *Appl. Phys. Lett.* **2007**, *91*, No. 093507.
(16) Kruger, M.; Buitelaar, M. R.; Nussbaumer, T.; Schonenberger, C.; Forro, L. *Appl. Phys. Lett.* **2001**, *78*, 1291.
(17) Rosenblatt, S.; Yaish, Y.; Park, J.; Gore, J.; Sazonova, V.; McEuen, P. L. *Nano Lett.* **2002**, *2*, 869.
(18) Das, A.; Pisana, S.; Chakraborty, B.; Piscanec, S.; Saha, S. K.; Waghmare, U. V.; Novoselov, K. S.; Krishnamurthy, H. R.; Geim, A. K.; Ferrari, A. C.; Sood, A. K. *Nat. Nanotechnol.* **2008**, *3*, 210.
(19) Heller, I.; Kong, J.; Williams, K. A.; Dekker, C.; Lemay, S. G. *J. Am. Chem. Soc.* **2006**, *128*, 7353.
(20) Heller, I.; Chatoor, S.; Männik, J.; Zevenbergen, M. A. G.; Dekker, C.; Lemay, S. G. *Phys. Status Solidi RRL* **2009**, *3*, 190.
(21) Adam, S.; Hwang, E. H.; Das Sarma, S. *Physica E* **2008**, *40*, 1022.
(22) Chen, J. H.; Jang, C.; Ishigami, M.; Xiao, S.; Cullen, W. G.; Williams, E. D.; Fuhrer, M. S. *Solid State Commun.* **2009**, *149*, 1080.
(23) Chen, F.; Xia, J. L.; Tao, N. J. *Nano Lett.* **2009**, *9*, 1621.
(24) Huard, B.; Stander, N.; Sulpizio, J. A.; Goldhaber-Gordon, D. *Phys. Rev. B* **2008**, *78*, 121402.
(25) Russo, S.; Craciun, M. F.; Yamamoto, M.; Morpurgo, A. F.; Tarucha, S. arXiv:0901.0485v1.

DOI: 10.1021/nl903665g | *Nano Lett.* **2010,** *10,* 1563--1567